International Journal of Modern Achievement in Science, Engineering and Technology (IJSET)
ISSN 3023-459X
DOI : 10.63053/ijset.5

Investigating the Elastic Response of Smart Cylinders Under Asymmetric Loading

Malihe Eftekhari [1]

1. Department of Mechanical Engineering, Sirjan University of Technology, Sirjan, Iran

ARTICLE INFO

Keywords: *Smart Cylinder, FGPM, Asymmetric Loading, Hygrothermo-Magneto-Elastic Response.*

ABSTRACT

This paper investigates the hygrothermal-magneto-elastic response of functionally graded piezomagnetic (FGPM) cylinders under asymmetric loading. The cylinders are supported by a Winkler-type elastic foundation, and their properties vary with the radius according to a power-law function. By solving 2D equations of Fickian diffusion and Fourier relations, the distribution of asymmetric moisture concentration and temperature field is determined. Incorporating constitutive equations into mechanical and magnetic equilibrium equations yields three second-order partial differential equations. The equations are solved using the separation of variables and complex Fourier series. Simulation results demonstrate the influence of hygrothermal loading, magnetic field, elastic foundation, and material inhomogeneity on the cylinder's response.

Introduction

Piezomagnetic materials, possessing both piezoelectric and magnetic characteristics, have garnered considerable attention due to their potential applications in aerospace, automotive, and biomedical industries for sensing and actuating purposes. Functionally graded materials (FGMs), characterized by spatially varying compositions enabling tailored mechanical, thermal, and electromagnetic properties, have also gained prominence. The combination of piezoelectric and FGM materials has led to the emergence of smart structures with exceptional properties. To effectively employ these smart structures in real-world scenarios, comprehending their response under diverse loading conditions is imperative.

Researchers have extensively investigated the diverse loading-induced behaviors of smart structures composed of piezoelectric and functionally graded materials (Sui et al., 2023; Yang et al., 2021). Dini et al. examined the effects of strain gradients and flexoelectricity on thermal stresses in micro-cylinders made of functionally graded piezoelectric materials (Dini et al., 2020; Hosseini et al., 2017). Galic and Horgan provided an exact solution for the axisymmetric problem of a piezoelectric cylinder subjected to internal pressure and electric loading (Galic & Horgan, 2003). Das et al. investigated stress and displacement fields in a FGM thick-walled sphere under constant interior and exterior pressure, using analytical and numerical models that account for radial variations in material properties (Das et al., 2023). Dai and Wang studied the thermo-electro-elastic behavior of a piezoelectric cylinder subjected to various loading conditions (Dai & Wang, 2006). Additionally, Khoshgoftar et al. analyzed the thermo-piezo-electric response of FG cylinders under thermal and mechanical loads (Khoshgoftar et al., 2009). Dini et al. presented analytical solutions for the magneto-thermo-elastic behavior of cylindrical and spherical pressure vessels, as well as three-layered sandwich disks made of FGMs, considering internal heat generation and convective boundary conditions (Dini et al., 2019; Hosseini & Dini, 2015; Nematollahi et al., 2019).

Several studies have investigated the behavior of FG and piezoelectric materials under various physical loadings (Fazelzadeh et al., 2011; Hosseini et al., 2019; Hosseini & Fazelzadeh, 2010; Hosseini et al., 2011; Rastgoo et al., 2017; Zandi-Baghche-Maryam et al., 2022). Chen et al. explored the 3D free vibration of FGPM cylinders containing compressible fluid and derived frequency equations based on 3D piezoelasticity exact equations using the state-space formulation (Chen et al., 2004). Jabbari et al. presented a general solution for the 3D thermal and mechanical stresses in FG cylinders, assuming power-law material properties and employing Bessel functions and Fourier series to solve the Navier equations (Jabbari et al., 2007). Shao et al. provided an exact solution for the thermomechanical behavior of FG cylinders under thermal and mechanical loadings using the Laplace transform method and complex Fourier series (Shao et al., 2008). Li et al. (2023) investigated the multi-field coupling of FG materials by analyzing the thermal distribution, displacement, strain, and stress of rotating FG cylinders or circular disks subjected to a uniform constant magnetic field (Li et al., 2023).

Allam et al. provided an analytical solution for the interaction of electric potentials, electric displacement, elastic deformations, and hygrothermal effects in hollow and solid cylinders made of functionally graded piezoelectric material (Allam et al., 2014). Dini and Abolbashari investigated the hygrothermo-electro-elastic response of cylinders composed of FGPM materials under non-axisymmetric thermal, mechanical, and electrical loadings (Dini & Abolbashari, 2016). Sayman conducted a stress analysis for multi-layered composite cylinders subjected to hygrothermal loading, considering both free-end and fixed-end boundary conditions (Sayman, 2005).

The behaviors of smart structures composed of piezoelectric and functionally graded materials have been extensively studied under various loading conditions. However, the specific investigation of the hygrothermal and electromagnetic loading effects on functionally graded piezomagnetic cylinders, considering the presence of an elastic foundation, remains limited. This manuscript aims to provide a comprehensive analysis of the behavior of such cylinders under hygrothermal and electromagnetic loading, taking into account the influence of an elastic foundation. The analysis focuses on asymmetric loading conditions to enhance the realism and applicability of the study to real-world scenarios.

1. Theoretical Formulation

The current investigation examines a FG piezomagnetic cylinder, which is subjected to mechanical, magnetic, and hygrothermal loads. The cylinder's inner and outer radii are denoted as a and b, respectively, and it is supported by a Winkler elastic foundation with a stiffness coefficient of k_w at its outer surface.

The material behavior of the piezomagnetic FG cylinder is modeled using linear constitutive equations that

account for the effects of hygrothermal, mechanical, and magnetic fields, as expressed in Eq. (1) (Arani et al., 2010; Saadatfar & Aghaie-Khafri, 2014).

$$\sigma_{rr} = C_{11}\frac{\partial u}{\partial r} + C_{12}\left[\frac{u}{r} + \frac{1}{r}\frac{\partial v}{\partial \theta}\right] + d_{11}\frac{\partial \psi}{\partial r} - \vartheta_1 T(r,\theta) - \varrho_1 \bar{C}(r,\theta)$$

$$\sigma_{\theta\theta} = C_{12}\frac{\partial u}{\partial r} + C_{22}\left[\frac{u}{r} + \frac{1}{r}\frac{\partial v}{\partial \theta}\right] + d_{21}\frac{\partial \psi}{\partial r} - \vartheta_2 T(r,\theta) - \varrho_2 \bar{C}(r,\theta)$$

$$\tau_{r\theta} = C_{31}\left[\frac{1}{r}\frac{\partial u}{\partial \theta} + \frac{\partial v}{\partial r} - \frac{v}{r}\right] + C_{12}\left[\frac{u}{r} + \frac{1}{r}\frac{\partial v}{\partial \theta}\right] + d_{31}\frac{1}{r}\frac{\partial \psi}{\partial \theta} \quad (1)$$

$$B_r = d_{11}\frac{\partial u}{\partial r} + d_{12}\left[\frac{u}{r} + \frac{1}{r}\frac{\partial v}{\partial \theta}\right] - g_{11}\frac{\partial \psi}{\partial r} + q_1 T(r,\theta) + \gamma_1 \bar{C}(r,\theta)$$

$$B_\theta = d_{31}\left[\frac{1}{r}\frac{\partial u}{\partial r} + \frac{\partial v}{\partial r} - \frac{v}{r}\right] - g_{22}\frac{1}{r}\frac{\partial \psi}{\partial \theta} + q_2 T(r,\theta) + \gamma_2 \bar{C}(r,\theta)$$

where σ_{ij} and B_i are stress and magnetic induction components, respectively. $\psi, C_{ij}, d_{ij}, \vartheta_i, \varrho_i, g_{ij}, p_i$, and γ_i are magnetic potential, elastic coefficient, piezomagnetic coefficient, thermal stress, hygroscopic stress, magnetic permeability, pyromagnetic coefficient, and hygromagnetic coefficient, respectively. Thermal and hygroscopic stresses are related to the elastic coefficient, thermal and moisture expansion coefficients as:

$$\vartheta_1 = C_{11}\alpha_r + C_{12}\alpha_\theta, \qquad \vartheta_2 = C_{12}\alpha_r + C_{22}\alpha_\theta$$
$$\varrho_1 = C_{11}\xi_r + C_{12}\xi_\theta, \qquad \varrho_2 = C_{12}\xi_r + C_{22}\xi_\theta \quad (2)$$

The equilibrium equations of a piezomagnetic cylinder, which take into account both mechanical and magnetic effects, can be expressed in terms of the radial and circumferential directions as follows:

$$\frac{\partial \sigma_{rr}}{\partial r} + \frac{1}{r}\frac{\partial \tau_{r\theta}}{\partial \theta} + \frac{\sigma_{rr} - \sigma_{\theta\theta}}{r} = 0$$
$$\frac{\partial \tau_{r\theta}}{\partial r} + \frac{1}{r}\frac{\partial \sigma_{\theta\theta}}{\partial \theta} + \frac{2}{r}\tau_{r\theta} = 0 \quad (3)$$
$$\frac{\partial B_r}{\partial r} + \frac{1}{r}\frac{\partial B_\theta}{\partial \theta} + \frac{B_r}{r} = 0$$

Equation (4) describes the mechanical, magnetic, and hygrothermal properties of the piezomagnetic cylinder, which are characterized by different non-homogeneity constants depending on the specific property under consideration (Akbarzadeh & Chen, 2013).

$$C_{ij} = C_{ij}^0 r^{\beta_1}, \quad d_{ij} = d_{ij}^0 r^{\beta_1}, \quad g_{ij} = g_{ij}^0 r^{\beta_1}$$
$$\vartheta_i = \vartheta_i^0 r^{\beta_1+\beta_2}, \quad \varrho_i = \varrho_i^0 r^{\beta_1+\beta_2}, \quad q_i = q_i^0 r^{\beta_1+\beta_2}, \quad \gamma_i = \gamma_i^0 r^{\beta_1+\beta_2} \quad (4)$$
$$k_i = k_i^0 r^{\beta_3}, \quad \omega_i = \omega_i^0 r^{\beta_3}$$

where β_1, β_2, and β_3 are the non-homogeneity constants of the material. Substituting Eqs. (1) and (4) into Eq. (3) results in three second-order partial differential equations that are coupled.

2. Heat Transfer and Moisture Diffusion Problem

The Fourier heat transfer equation in steady-state, without any internal heat generation, for a 2D problem in cylindrical coordinates is expressed below along with the general boundary conditions (Sih G.C., 1986).

$$\frac{1}{r}\frac{\partial}{\partial r}\left(rK_r\frac{\partial T}{\partial r}\right) + \frac{1}{r^2}\frac{\partial}{\partial \theta}\left(K_\theta\frac{\partial T}{\partial \theta}\right) = 0$$
$$Q_{11}T(a,\theta) + Q_{12}\frac{\partial T(a,\theta)}{\partial r} = f_1(\theta) \quad (5)$$
$$Q_{21}T(b,\theta) + Q_{22}\frac{\partial T(b,\theta)}{\partial r} = f_2(\theta)$$

where K_r and K_θ expressed by Eq. (4) are the thermal conductivity coefficients. Q_{ij} represents the constant

thermal parameters associated with the conduction and convection coefficients. Functions $f_1(\theta)$ and $f_2(\theta)$ are given functions in the inner and outer radius, respectively. Simplifying Eq. (5) yields:

$$r^2\frac{\partial^2 T}{\partial r^2}+r(\beta_3+1)\frac{\partial T}{\partial r}+\frac{\partial^2 T}{\partial \theta^2}=0 \tag{6}$$

The steady-state 2D equation governing Fickian moisture diffusion in a functionally graded piezomagnetic cylinder can be expressed in cylindrical coordinates, along with the general boundary conditions, as follows (Sih G.C., 1986):

$$\frac{1}{r}\frac{\partial}{\partial r}\left(r\,\omega_r\frac{\partial \bar{C}}{\partial r}\right)+\frac{1}{r^2}\frac{\partial}{\partial \theta}\left(\omega_\theta\frac{\partial \bar{C}}{\partial \theta}\right)=0$$

$$Z_{11}\bar{C}(a,\theta)+Z_{12}\frac{\partial \bar{C}(a,\theta)}{\partial r}=h_1(\theta) \tag{7}$$

$$Z_{21}\bar{C}(b,\theta)+Z_{22}\frac{\partial \bar{C}(b,\theta)}{\partial r}=h_2(\theta)$$

In Eq. (7), ω_r and ω_θ are the moisture diffusion, and vary according to Eq. (4) along the cylinder thickness. Z_{ij} represents the constant parameters related to moisture, and $h_1(\theta)$ and $h_2(\theta)$ are given functions at the inner and outer radii, respectively. To solve Eqs. (6, 7), the complex Fourier series method can be employed.

By solving Eqs. (1-7) we can obtained, displacments, stresses and magnetic induction components

3. Numerical results

This section presents numerical results for functionally graded piezomagnetic cylinders with thick walls that are supported by a Winkler-type elastic foundation. The cylinder is made of piezomagnetic materials (BaTiO3/CoFe2O4) (Akbarzadeh & Chen, 2012; Saadatfar & Aghaie-Khafri, 2015). The cylinder is subjected to internal pressure and rests on the foundation at its outer surface.

Figs. 1-3 show the effects of different parameters on the behavior of the cylinder for the second set of boundary conditions. Fig. 1 illustrates the influence of the non-homogeneity constant on the distribution of displacement, stresses, and magnetic potential at $\theta=\pi/3$, assuming $k_w=10^9\ N/m^3$ and $\beta_1=\beta_2=\beta_3=\beta$. Fig. 1a indicates that the radial stress decreases with an increase in the non-homogeneity constant. In Fig. 1b, it can be observed that the circumferential stress decreases and increases in the ranges of $\frac{r}{a}<1.14$ and $\frac{r}{a}>1.14$, respectively, by increasing the non-homogeneity constant. Based on Fig. 1c, increasing the non-homogeneity constant results in an increase in the shear stress. The maximum shear stress is observed near the radius $\frac{r}{a}=1.1$. Finally, Fig. 1d shows that the magnetic potential increases as the non-homogeneity constant increases.

b *a*

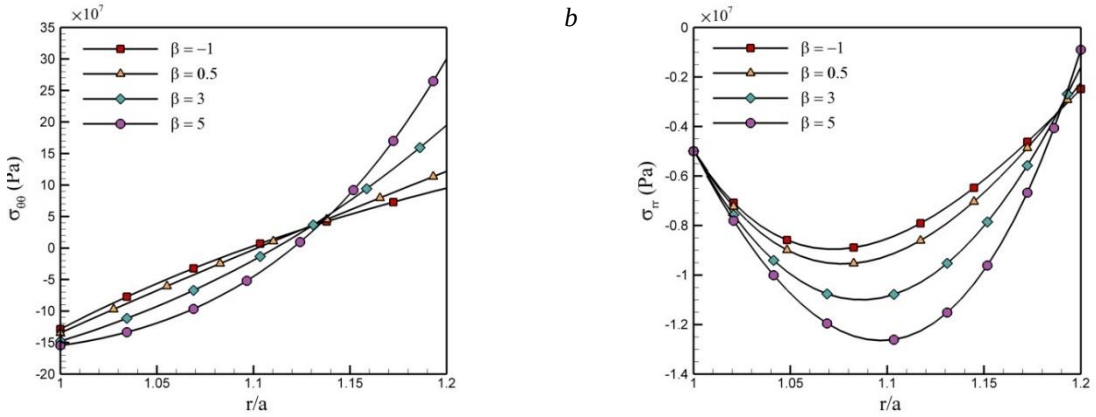

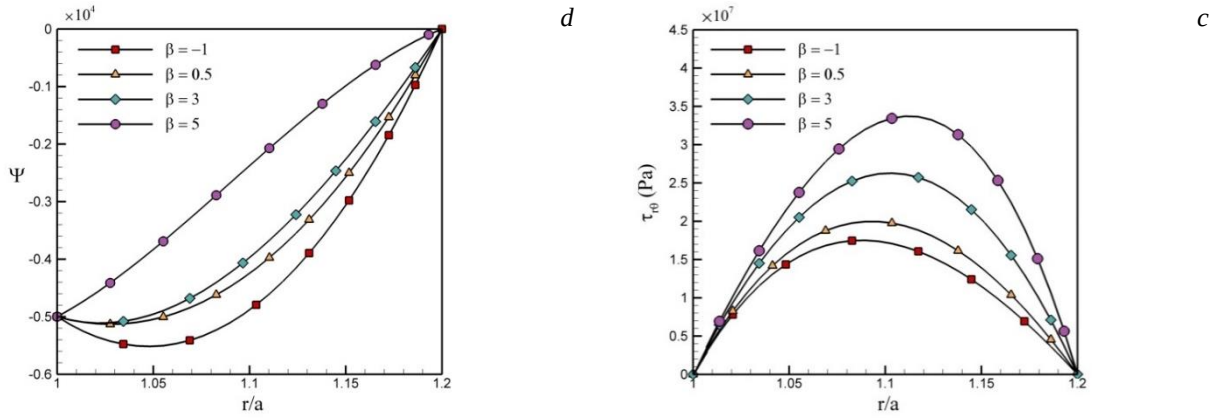

Fig. 1. Distribution of a) radial stress, b) circumferential stress, c) shear stress, d) magnetic potential for different non-homogeneity constant in the FGPM cylinder, ($\theta = \pi/3, k_w = 10^9\ N/m^3$).

Fig. 2 illustrates the impact of hygrothermal loading on the distribution of displacement, stresses, and magnetic potential at $\theta = \pi/3$, assuming $k_w = 10^9\ N/m^3$ and $\beta_1 = \beta_2 = \beta_3 = \beta = 0.5$. Fig. 2a indicates that the radial stresses decrease as the hygrothermal loading increases. In Fig. 2b, it can be realized that an increase in hygrothermal loading results in a decrease and increase in circumferential stress at $\frac{r}{a} < 1.11$ and $\frac{r}{a} > 1.11$, respectively. As shown in Fig. 2c, an increase in hygrothermal loading leads to an increase in shear stress, whereas Fig. 2d shows that the magnetic potential decreases with increasing hygrothermal loading.

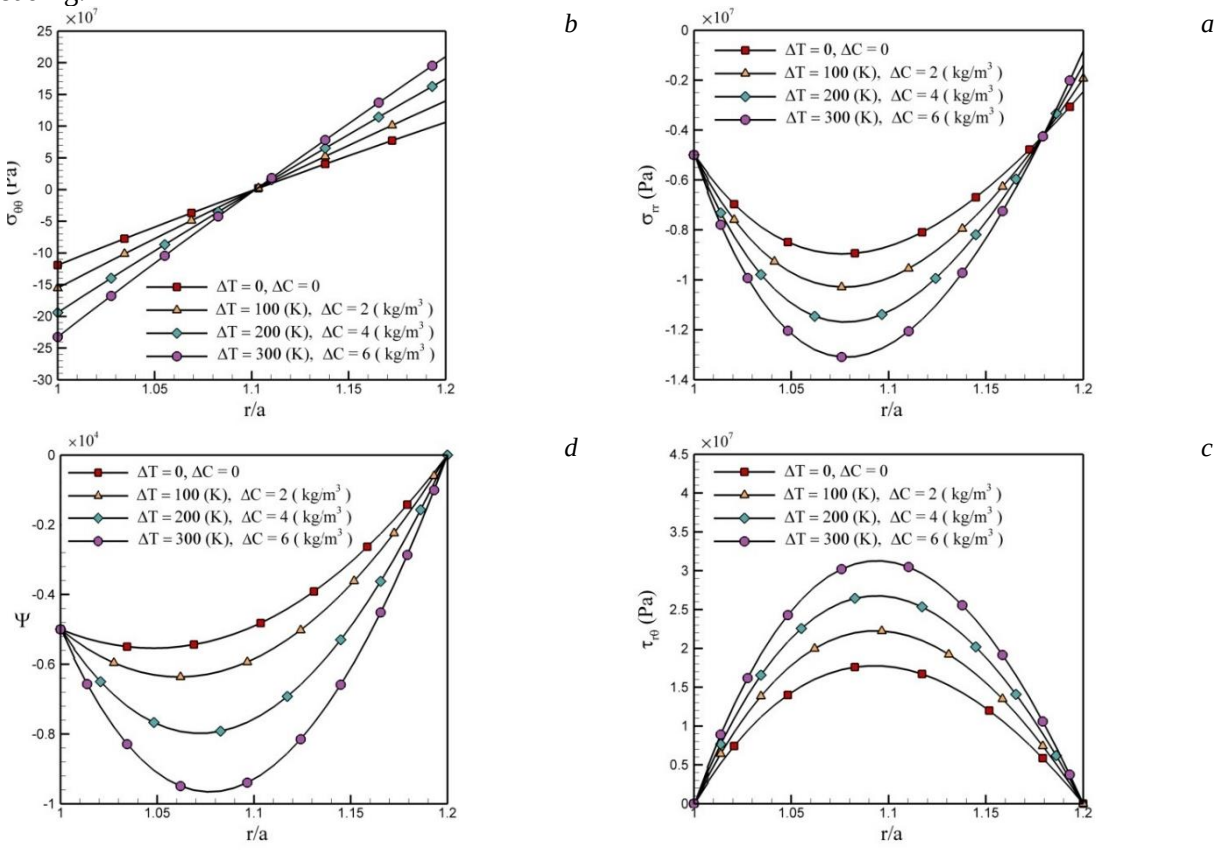

Fig. 2. Distribution of a) radial stress, b) circumferential stress, c) shear stress, d) magnetic potential for hygro-thermal loading in the FGPM cylinder, ($\beta = 0.5, \theta = \pi/3\ , k_w = 10^9\ N/m^3$).

Fig. 3 depicts the impact of elastic foundation stiffness on the distribution of displacement, stresses, and magnetic potential at $\theta = \pi/3$, assuming $\beta_1 = \beta_2 = \beta_3 = \beta = 0.5$. In Fig. 3a, it can be observed that increasing the stiffness of the elastic foundation causes an increase in radial stresses along the cylinder thickness. Moreover, at the outer surface of the cylinder $\frac{r}{a} = 1.2$ and $\theta = \pi/3$, increasing the stiffness of

the elastic foundation decreases the absolute value of the radial stress. Based on Fig. 3b, the circumferential stress increases at $\frac{r}{a} < 1.11$ and decreases at $\frac{r}{a} > 1.11$ by increasing the stiffness of the elastic foundation. Figs. 3c and 3d indicate that the shear stress and magnetic potential, respectively, decrease and increase with increasing stiffness of the elastic foundation.

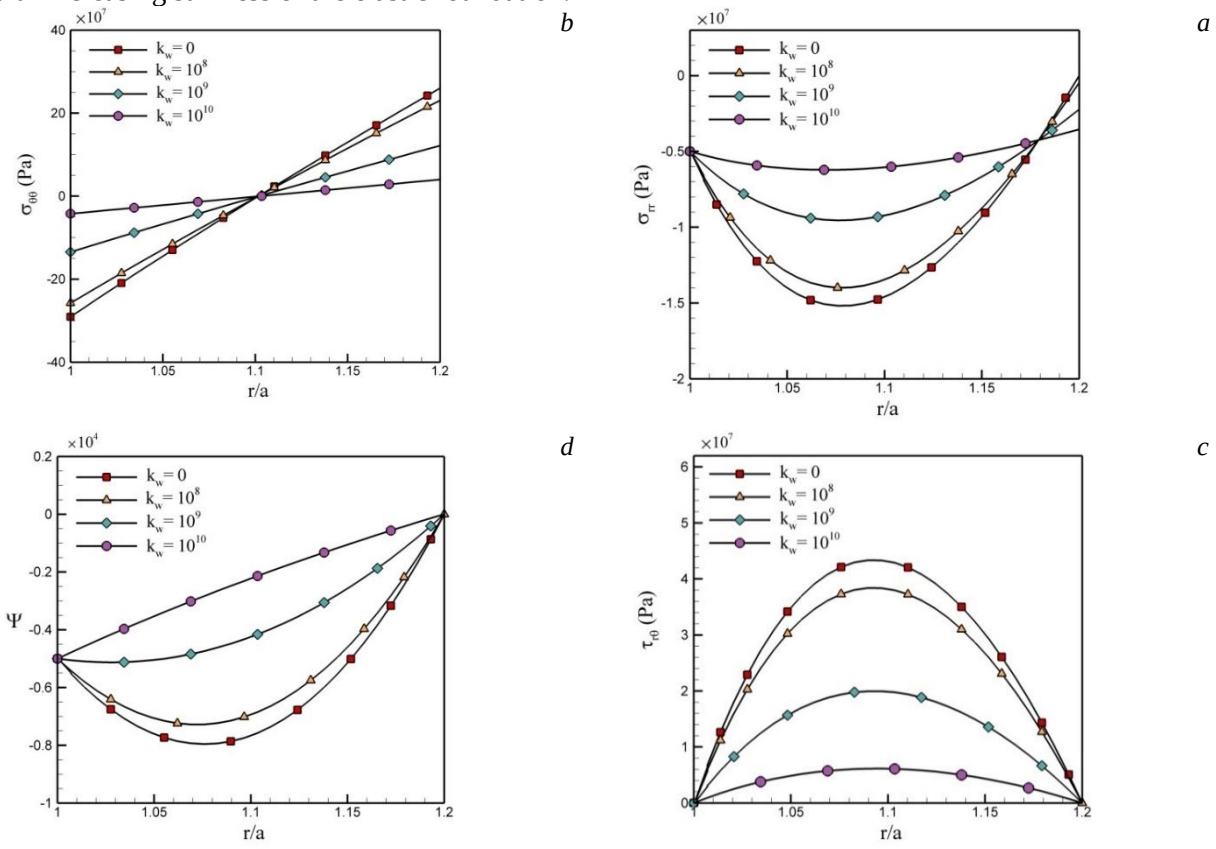

Fig. 3. Distribution of a) radial stress, b) circumferential stress, c) shear stress, d) magnetic potential for elastic foundation stiffness in the FGPM cylinder, ($\beta = 0.5, \theta = \pi/3$).

4. Conclusion

In this study, hygrothermal stresses in thick-walled cylinders made of functionally graded piezomagnetic materials were investigated considering elastic foundation and asymmetric loadings. The mechanical, hygrothermal, electrical, and magnetic properties were assumed to be a function of the radius of the cylinder according to the power law. The distributions of temperature and moisture concentration were computed using 2D equations of Fourier heat transfer and Fickian moisture diffusion. The coupled partial differential equations were solved using the method of separation of variables and the complex Fourier series. Numerical simulations were obtained for a certain angle to investigate the effects of hygrothermal loading, elastic foundation, and non-homogeneity constant. Based on the results and analysis of the diagrams, the following conclusions were made in this study:

1. The non-homogeneity constant has significant effects on the distribution of stresses, magnetic potential, temperature, and moisture concentration in the thick-walled cylinder. In addition, when $\beta_1 = \beta_2 = \beta_3 = \beta$, increasing the non-homogeneity constant in the range of $\beta > 0$ leads to a decrease in the absolute values of radial stress, and magnetic potential, while the decrement of non-homogeneity constant in the range of $\beta < 0$ increases the above-mentioned parameters.
2. Hygrothermal loading has remarkable effects on the distribution of stresses, and magnetic potential. Increasing temperature and moisture concentration simultaneously lead to a decrease in radial stress and an increase in shear stress.
3. Increasing the stiffness of the elastic foundation leads to a decrease in shear stress, and an increase in radial stress and magnetic potential along the cylinder thickness. Moreover, the radial stress at the outer surface $\frac{r}{a} = 1.2$ decreases with increasing the stiffness of the elastic foundation. The circumferential

stress usually increases at $\frac{r}{a} < 1.11$ and decreases at $\frac{r}{a} > 1.11$ by increasing the stiffness.

References

1. Akbarzadeh, A., & Chen, Z. (2012). Magnetoelectroelastic behavior of rotating cylinders resting on an elastic foundation under hygrothermal loading. Smart Materials and Structures, 21(12), 125013.
2. Akbarzadeh, A., & Chen, Z. (2013). Hygrothermal stresses in one-dimensional functionally graded piezoelectric media in constant magnetic field. Composite Structures, 97, 317-331.
3. Allam, M., Zenkour, A., & Tantawy, R. (2014). Analysis of functionally graded piezoelectric cylinders in a hygrothermal environment. Advances in Applied Mathematics and Mechanics, 6(2), 233-246.
4. Arani, A. G., Maraghi, Z. K., Mozdianfard, M., & Shajari, A. (2010). Thermo-piezo-magneto-mechanical stresses analysis of FGPM hollow rotating thin disk. International Journal of Mechanics and Materials in Design, 6(4), 341-349.
5. Chen, W., Bian, Z., Lv, C., & Ding, H. (2004). 3D free vibration analysis of a functionally graded piezoelectric hollow cylinder filled with compressible fluid. International Journal of Solids and Structures, 41(3-4), 947-964.
6. Dai, H., & Wang, X. (2006). Magneto–thermo–electro–elastic transient response in a piezoelectric hollow cylinder subjected to complex loadings. International Journal of Solids and Structures, 43(18-19), 5628-5646.
7. Das, P., Islam, M. A., Somadder, S., & Hasib, M. A. (2023). Analytical and numerical solutions of pressurized thick-walled FGM spheres. Archive of Applied Mechanics, 93(7), 2781-2792. https://doi.org/10.1007/s00419-023-02406-3
8. Dhore, N., Khalsa, L., & Varghese, V. (2023). Hygrothermoelastic analysis of non-simple nano-beam induced by ramp-type heating. Archive of Applied Mechanics. https://doi.org/10.1007/s00419-023-02444-x
9. Dini, A., & Abolbashari, M. H. (2016). Hygro-thermo-electro-elastic response of a functionally graded piezoelectric cylinder resting on an elastic foundation subjected to non-axisymmetric loads. International Journal of Pressure Vessels and Piping, 147, 21-40.
10. Dini, A., Nematollahi, M. A., & Hosseini, M. (2019). Analytical solution for magneto-thermo-elastic responses of an annular functionally graded sandwich disk by considering internal heat generation and convective boundary condition. Journal of Sandwich Structures & Materials, 1099636219839161.
11. Dini, A., Shariati, M., Zarghami, F., & Nematollahi, M. A. (2020). Size-dependent analysis of a functionally graded piezoelectric micro-cylinder based on the strain gradient theory with the consideration of flexoelectric effect: plane strain problem. Journal of the Brazilian Society of Mechanical Sciences and Engineering, 42(8), 1-22.
12. El Khouddar, Y., Adri, A., Outassafte, O., El Hantati, I., Rifai, S., & Benamar, R. (2022). Influence of hygro-thermal effects on the geometrically nonlinear free and forced vibrations of piezoelectric functional gradient beams with arbitrary number of concentrated masses. Archive of Applied Mechanics, 92(9), 2767-2784. https://doi.org/10.1007/s00419-022-02219-w
13. Fazelzadeh, S. A., Hosseini, M., & Madani, H. (2011). Thermal divergence of supersonic functionally graded plates. Journal of thermal Stresses, 34(8), 759-777.
14. Galic, D., & Horgan, C. (2003). The stress response of radially polarized rotating piezoelectric cylinders. J. Appl. Mech., 70(3), 426-435.
15. Hosseini, M., Arani, A. G., Karamizadeh, M. R., Afshari, H., & Niknejad, S. (2019). Aeroelastic analysis of cantilever non-symmetric FG sandwich plates under yawed supersonic flow. Wind and Structures, 29(6), 457.
16. Hosseini, M., & Dini, A. (2015). Magneto-thermo-elastic response of a rotating functionally graded cylinder. Structural Engineering and Mechanics, 56(1), 137-156. https://doi.org/10.12989/sem.2015.56.1.137
17. Hosseini, M., Dini, A., & Eftekhari, M. (2017). Strain gradient effects on the thermoelastic analysis of a functionally graded micro-rotating cylinder using generalized differential quadrature method. Acta Mechanica, 228(5), 1563-1580.
18. Hosseini, M., & Fazelzadeh, S. (2010). Aerothermoelastic post-critical and vibration analysis of temperature-dependent functionally graded panels. Journal of thermal Stresses, 33(12), 1188-1212.
19. Hosseini, M., Fazelzadeh, S., & Marzocca, P. (2011). Chaotic and bifurcation dynamic behavior of functionally graded curved panels under aero-thermal loads. International Journal of Bifurcation and Chaos, 21(03), 931-954.
20. Jabbari, M., Mohazzab, A., Bahtui, A., & Eslami, M. (2007). Analytical solution for three-dimensional stresses in a short length FGM hollow cylinder. ZAMM-Journal of Applied Mathematics and Mechanics/Zeitschrift für Angewandte Mathematik und Mechanik: Applied Mathematics and Mechanics, 87(6), 413-429.
21. Khoshgoftar, M., Arani, A. G., & Arefi, M. (2009). Thermoelastic analysis of a thick walled cylinder made of functionally graded piezoelectric material. Smart Materials and Structures, 18(11), 115007.
22. Li, X., Xie, J., & Shi, P. (2023). Magneto-thermal–mechanical analysis of functionally graded rotating cylinder and circular disk. Archive of Applied Mechanics, 93(4), 1449-1457. https://doi.org/10.1007/s00419-022-02338-4
23. Nematollahi, M., Dini, A., & Hosseini, M. (2019). Thermo-magnetic analysis of thick-walled spherical

pressure vessels made of functionally graded materials. Applied Mathematics and Mechanics, 40(6), 751-766.
24. Rastgoo, M., Fazelzadeh, S. A., Eftekhari, M., & Hosseini, M. (2017). Flow-induced flutter instability of functionally graded cantilever pipe. International Journal of Acoustics and Vibration, 22(3), 320-325.
25. Saadatfar, M., & Aghaie-Khafri, M. (2014). Hygrothermomagnetoelectroelastic analysis of a functionally graded magnetoelectroelastic hollow sphere resting on an elastic foundation. Smart Materials and Structures, 23(3), 035004.
26. Saadatfar, M., & Aghaie-Khafri, M. (2015). Hygrothermal analysis of a rotating smart exponentially graded cylindrical shell with imperfect bonding supported by an elastic foundation. Aerospace Science and Technology, 43, 37-50.
27. Sayman, O. (2005). Analysis of multi-layered composite cylinders under hygrothermal loading. Composites Part A: Applied Science and Manufacturing, 36(7), 923-933. https://doi.org/10.1016/j.compositesa.2004.12.007
28. Shao, Z., Ang, K., Reddy, J., & Wang, T. (2008). Nonaxisymmetric thermomechanical analysis of functionally graded hollow cylinders. Journal of thermal Stresses, 31(6), 515-536.
29. Sih G.C., M., J.G., Chou S.C. (1986). Hygrothermoelasticity. Dordrecht: Martinus Nijhoff Publishers.
30. Sui, Y., Wang, W., Zhang, H., & Liang, H. (2023). 3D frictional contact of graded magneto-electro-elastic film-substrate system under electromagnetic fields. International Journal of Solids and Structures, 269, 112217. https://doi.org/https://doi.org/10.1016/j.ijsolstr.2023.112217
31. Wang, Y., Xu, R., Ding, H., & Chen, J. (2010). Three-dimensional exact solutions for free vibrations of simply supported magneto-electro-elastic cylindrical panels. International Journal of Engineering Science, 48(12), 1778-1796. https://doi.org/10.1016/j.ijengsci.2010.09.022
32. Yang, J., Sun, G., & Yang, J. (2021). Bifurcation and chaos of functionally graded carbon nanotube reinforced composite beam with piezoelectric layer. Advances in Applied Mathematics and Mechanics, 13(3), 569-589.
33. Zandi-Baghche-Maryam, A., Dini, A., & Hosseini, M. (2022). Wave propagation analysis of inhomogeneous Multi–Nanoplate systems subjected to a thermal field considering surface and flexoelectricity effects. Waves in Random and Complex Media, 1-28.